

ST. NO. R8513
U.D.C.
ADH. *al*

R. & M. No. 2512
(5852, 8458)
A.R.C. Technical Report



MINISTRY OF SUPPLY

AERONAUTICAL RESEARCH COUNCIL
REPORTS AND MEMORANDA

The Ideal Drag Due to a Shock Wave

Parts I and II

By

C. N. H. LOCK, M.A., F.R.A.E.S.,
of the Aerodynamics Division, N.P.L.

Crown Copyright Reserved

LONDON : HIS MAJESTY'S STATIONERY OFFICE

1951

PRICE 4s 6d NET

STACK FILE



The Ideal Drag Due to a Shock Wave*

By

C. N. H. LOCK, M.A., F.R.A.E.S.,
of the Aerodynamics Division, N.P.L.



Reports and Memoranda No. 2512

19th February, 1945

PART I

1. *Introduction.*—The subject of the present note is the increase of the drag of an aerofoil which arises from the presence of limited shock waves when the forward speed lies between the so-called shock stalling speed and the velocity of sound. Evidence from photographs and other sources shows that under certain conditions a single limited shock wave exists on one or both surfaces of an aerofoil when the local speed at some point of the surface exceeds the velocity of sound. It is therefore suggested that ideal two-dimensional motions about an aerofoil may exist, which satisfy the equations of motion of a non-viscous non-conducting compressible fluid, at all points of the field outside a limited shock wave attached to one or both surfaces of the aerofoil. The shock wave is to be considered merely as a surface of discontinuity across which the usual conditions of continuity of flow, momentum, total energy and velocity parallel to the surface, are satisfied; it forms the rear boundary of a limited region in which the flow is supersonic and its intensity falls to zero at its outer edge where the velocity is equal to the local velocity of sound.

As a result of the increase of entropy on passing through the shock wave, the density and velocity at a large distance behind the aerofoil of a particle of fluid that has passed through the shock wave will both be reduced below their free-stream values; the pressure will have regained its free-stream value. The ordinary momentum integrals taken across lines far in front of, and far behind, the aerofoil thus determine the drag in the ideal case; this may be considered as the ideal (lowest possible) drag due to an actual shock wave.

2. *Ideal Drag.*—The object of the present note is to point out the possibility of converting the momentum integral into an integral taken over the surface of the shock waves (one or two). In the notation of Fig. 1a, u and v denote velocity components parallel and perpendicular to the shock wave and q their resultant; suffix 0 denotes free-stream values (V , free-stream velocity); suffixes 1 and 2 denote conditions just upstream and just downstream of the shock wave, suffix 3 denotes conditions in the wake far behind the aerofoil. The ordinary momentum integral for drag is

$$D = \int (V - q_3) \rho_3 q_3 d\sigma_3 \quad \dots \dots \dots (1)$$

per unit length, where $d\sigma$ denotes an element of length normal to a stream tube which in this case is normal to the free stream. Let ds be an element of length (measured along the surface

* The method of the present report, leading to the curves of Fig. 2, was developed early in 1939, but the paper has been rewritten as a result of the advice of Mr. A. D. Young whose suggestions are gratefully acknowledged.

of the two-dimensional shock wave C) containing the same stream tube as $d\sigma_3$. Then by continuity

$$\begin{aligned} \rho_3 q_3 d\sigma_3 &= \rho_2 q_2 d\sigma_2, \\ &= \rho_2 u_2 ds, \\ &= m ds, \end{aligned}$$

where $m = \rho_1 u_1 = \rho_2 u_2$.

If E be the total energy per unit mass, which is assumed to be constant throughout the fluid,

$$E = \frac{1}{2} q_3^2 + \frac{\gamma}{\gamma - 1} \frac{p_0}{\rho_3} = \frac{1}{2} V^2 + \frac{\gamma}{\gamma - 1} \frac{p_0}{\rho_0} \dots \dots \dots (2)$$

Again since the conditions are assumed to be isentropic along the stream tube from section (2) to section (3),

$$\frac{p_2}{\rho_2^\gamma} = \frac{p_3}{\rho_3^\gamma} = \frac{p_0}{\rho_0^\gamma} \dots \dots \dots (3)$$

Hence
$$\frac{1}{2}(V^2 - q_3^2) = \frac{\gamma}{\gamma - 1} \frac{p_0}{\rho_0} \left\{ \left(\frac{\rho_1}{\rho_2}\right) \left(\frac{p_2}{p_1}\right)^{1/\gamma} - 1 \right\} \dots \dots \dots (4)$$

If S is the entropy, given by

$$\exp. (S/C_v) = p/\rho^\gamma \dots \dots \dots (5)$$

for a perfect gas,

$$\begin{aligned} \left(\frac{\rho_1}{\rho_2}\right) \left(\frac{p_2}{p_1}\right)^{1/\gamma} &= F \text{ (definition of } F) \\ &= \exp. \{(S_2 - S_1)/\gamma C_v\} \dots \dots \dots (6) \end{aligned}$$

Finally equation (1) may be transformed into

$$D = V \int m ds \left\{ 1 - \left[1 - \frac{2}{(\gamma - 1) M_0^2} (F - 1) \right]^{1/2} \right\} \dots \dots \dots (7)$$

taken over the whole surface of one or both shock waves, where

$$M_0^2 = \frac{\rho_0 V^2}{\gamma p_0}$$

is the Mach number of the free stream. It may be shown that

$$\frac{\rho_1}{\rho_2} = \frac{(\gamma + 1) p_1 + (\gamma - 1) p_2}{(\gamma - 1) p_1 + (\gamma + 1) p_2},$$

and so

$$F = \frac{(\gamma + 1) p_1 + (\gamma - 1) p_2}{(\gamma - 1) p_1 + (\gamma + 1) p_2} \left(\frac{p_2}{p_1}\right)^{1/\gamma}, \dots \dots \dots (8)$$

and F can be evaluated in a practical case if p_1 and p_2 are both measured. The value of m , however, requires the determination of u_1 or of the inclination of the shock wave to the stream. The latter may be determined if p_1 and p_2 are both known.

It is proposed to attempt the measurement of p_1 and p_2 over the surface of shock waves on a 5-in. chord aerofoil in the rectangular high-speed tunnel, to attempt to evaluate the integral (7) for the ideal drag, and to compare it with the drag deduced from wake exploration and with the form drag deduced from pressure measurement over the surface.

3. *Use of Low-speed Potential Flow.*—A method will now be described of evaluating the drag integral (7) in terms of the known low-speed potential flow round a body of given shape on the basis of certain crude assumptions. Assume that the shock wave starts from the point of low-speed maximum velocity N (Fig. 1b) and lies along a line of constant velocity potential NP (everywhere normal to the streamlines). Let s be the distance along the curve measured from N to an arbitrary point P . Write

$$p_{cL} = \frac{p_{0L} - p_L}{\frac{1}{2}\rho_{0L} V_L^2} \quad \dots \quad (9)$$

at the point P where p_L and V_L stand for low-speed potential (incompressible) values; then p_{cL} may be considered as a known function of s . At any Mach number M_0 above the critical value, if p_1 is the pressure at P just in front of the shock wave it will be assumed that

$$\frac{p_0 - p_1}{\frac{1}{2}\rho_0 V^2} = \phi(M_0) p_{cL}, \quad \dots \quad (10)$$

where $\phi(M_0)$ is a function of M_0 only, which will be taken here to be equal to the Glauert factor

$$\phi(M_0) = (1 - M_0^2)^{-1/2*} \quad \dots \quad (11)$$

Equation (10) may be written in the form

$$\frac{p_1}{p_0} = 1 - \frac{1}{2}\gamma M_0^2 \phi(M_0) p_{cL}, \quad \dots \quad (12)$$

and (using the ordinary relations of constant energy and entropy) it follows that

$$1 + \frac{1}{2}(\gamma - 1) M_1^2 = \left\{1 + \frac{1}{2}(\gamma - 1) M_0^2\right\} \left(\frac{p_1}{p_0}\right)^{\frac{\gamma-1}{\gamma}}, \quad \dots \quad (13)$$

since the shock wave is everywhere normal to the local stream lines. The critical Mach number M_{c0} is equal to the value of M_0 given by substituting in equation (13), $M_1 = 1$ and p_{cL} equal to its value p_{cLN} at the point N .

To express the integral in equation (7) for the drag as a function of M_0 (ρ_0 , V_0) and p_{cL} only we make use of the relations

$$\begin{aligned} \frac{m}{\rho_0 V} &= \frac{\rho_1 u_1}{\rho_0 V} \\ &= \frac{M_1}{M_0} \left\{1 - \frac{1}{2}\gamma M_0^2 \phi p_{cL}\right\}^{\frac{\gamma+1}{2\gamma}}, \quad \dots \quad (14) \end{aligned}$$

using (13), and the known relation

$$\frac{p_2}{p_1} = \frac{2\gamma}{\gamma + 1} M_1^2 - \frac{\gamma - 1}{\gamma + 1}, \quad \dots \quad (15)$$

F being given by equation (8) and M_1 by equations (13) and (12).

* This assumption is made by Jacobs in his formula for the critical Mach number.

The drag may then be evaluated, for any value of M_0 greater than M_{c0} , by equation (7), the range of integration being from the surface of the aerofoil to the point Q (Fig. 1b) at which $s = s_Q$ and $M_1 = 1$, the value p_{cLQ} of p_{cL} being determined by substituting $M_1 = 1$ and $p_{cL} = p_{cLQ}$ in equation (13).

4. *First Order Theory.*—It is of some interest to establish in a general manner the order of magnitude of the drag given by the above equations for a Mach number M_0 which exceeds the critical Mach number M_{c0} by an amount

$$\lambda = M_0 - M_{c0},$$

which is considered as a small quantity. It will be shown that on the basis of the above assumptions, s_Q is in general of order λ , while it is known that $(F - 1)$ is of order $\{(p_2/p_1) - 1\}^3$ or λ^3 , and so the drag is of order λ^4 .

Again the assumption that the shock wave coincides with the equipotential through the point of maximum suction is not likely to be true in the limit for small values of λ if a shock wave is formed immediately M_0 exceeds M_{c0} . Hence the conclusion that the ideal drag is of order not greater than λ^4 will in fact hold for the ideal case.

In Appendix I the relation

$$C_D = K\lambda^4 + 0(\lambda^5) \quad \dots \quad (16)$$

is deduced from the previous equations, and K is expressed as a function of M_{c0} , p_{cLN} and α where

$$p_{cL} = p_{cLN} - \alpha s + 0(s^2) \quad \dots \quad (17)$$

Also M_{c0} is a known function of p_{cLN} , being the value of M_0 given by putting $M_1 = 1$ and $p_{cL} = p_{cLN}$ in equation (13).

In Appendix II K is evaluated for the case of an elliptic cylinder at zero incidence for which it is necessary to write

$$C_D = 2K\lambda^4, \quad \dots \quad (18)$$

since there will be two symmetrical shock waves.

Curves of C_D deduced from formula (18) are plotted in Fig. 2 for a series of values of the critical Mach number M_c corresponding to a series of values of thickness ratio of the elliptic cylinder (Table 1). On the same figure are plotted a selection of curves of C_D for certain aerofoils deduced from pitot traverse observations in the N.P.L.* High Speed Tunnel and a single curve of form-drag coefficient deduced from observations of pressure in the N.A.C.A.† 24-in High Speed Tunnel. No special significance is attached to this comparison except to bring out the point that even if a shock wave is always formed immediately the velocity of sound is first exceeded on the surface, the rise in drag to be expected apart from boundary-layer effects will be very small at first, being in general of the fourth order of the intensity of the shock wave.

* N.P.L. National Physical Laboratory, Great Britain.

† N.A.C.A. National Advisory Committee for Aeronautics, U.S.A.

APPENDIX I

Write $M_1 = 1 + \mu_1$,

and consider equations (13) and (12) as defining μ_1 as a function of M_0 and p_{cL} in the form

$$\mu_1 = \mu_1(M_0, p_{cL}), \quad \dots \quad (A1)$$

Then by definition of M_{c0} , p_{cLN} and p_{cLQ} ,

$$0 = \mu_1(M_{c0}, p_{cLN}), \quad \dots \quad (A2)$$

$$0 = \mu_1(M_0, p_{cLQ}). \quad \dots \quad (A3)$$

Assume that μ_1 is small; then s_Q is a small quantity of order μ_1 and we can write

$$p_{cL} = p_{cLN} - \alpha s + O(s^2), \quad \dots \quad (A4)$$

$$p_{cLQ} = p_{cLN} - \alpha s_Q + O(s_Q^2), \quad \dots \quad (A5)$$

where α is a constant derivable from the known low-speed motion. Write μ_{1M}, μ_{1p} as abbreviations for the result of putting $M_0 = M_{c0}, p_{cL} = p_{cLN}$ in $\partial\mu_1/\partial M_0, \partial\mu_1/\partial p_{cL}$ respectively, after differentiation. Then (A1), (A2) and (A3) give

$$\mu_1 = \lambda\mu_{1M} - \alpha s\mu_{1p},$$

$$0 = \lambda\mu_{1M} - \alpha s_Q\mu_{1p},$$

and so

$$\mu_1 = \alpha\mu_{1p}(s_Q - s),$$

with

$$s_Q = \frac{\lambda\mu_{1M}}{\alpha\mu_{1p}}.$$

By differentiating (13) with (12) we have

$$\mu_{1M} = \frac{1}{2}(\gamma + 1) M_{c0} \left\{ \frac{1}{1 + \frac{1}{2}(\gamma - 1)M_{c0}^2} + \frac{1}{2} \left(\frac{p_0}{p_1} \right)_N p_{cLN} (2\phi + M_{c0}\phi') \right\},$$

$$\mu_{1p} = \left(\frac{1}{4} \right) (\gamma + 1) \left(\frac{p_0}{p_1} \right)_N M_{c0}^2 \phi,$$

where

$$\left(\frac{p_1}{p_0} \right)_N = 1 - \frac{1}{2}\gamma M_{c0}^2 \phi p_{cLN}.$$

It may be shown that to the first order equations (8) and (12) give

$$F - 1 = \frac{16}{3} \frac{\gamma - 1}{(\gamma + 1)^2} \mu_1^3,$$

and that

$$\frac{m}{\rho_0 V} = \left(\frac{p_1}{p_0} \right)_N^{\frac{\gamma+1}{2\gamma}} / M_{c0}.$$

Substitution in equation (7) gives to the first order

$$C_D = \frac{D}{\frac{1}{2}\rho_0 V_c^2},$$

$$= \int_0^{s_0} \left(\frac{p_1}{p_0}\right)_N^{\gamma+1} \frac{32}{3(\gamma+1)^2} \left(\frac{\alpha\mu_1 p}{M_{c0}}\right)^3 (s_0 - s)^3 \frac{ds}{c},$$

$$= K\lambda^4,$$

where

$$\alpha c K = \frac{2(\gamma+1)(p_1/p_0)_N^{(3\gamma+1)/2\gamma}}{3M_{c0}\phi(M_{c0})} \left\{ \frac{1}{1 + \frac{1}{2}(\gamma-1)M_{c0}^2} + \left(\frac{p_0}{p_1}\right)_N p_{cLN} \left(\phi + \frac{1}{2}M_{c0}\phi'\right)^4 \right\},$$

which is a function of M_{c0} and p_{cLN} only, and M_{c0} is a known function of p_{cLN} (Table 1). On the assumption that

$$\phi = (1 - M_{c0}^2)^{1/2},$$

the factor $\phi + \frac{1}{2}M_{c0}\phi' = \phi^3 (1 - \frac{1}{2}M_{c0}^2)$.

APPENDIX II

For an elliptic cylinder of fineness ratio τ at zero incidence, it may be shown that

$$p_{cLN} = (2 + \tau),$$

$$\alpha c = 4(1 + \tau)^2 \tau,$$

and the value of K is to be doubled since there are two shock waves (Table 1).

TABLE 1

General			Elliptic cylinder at zero incidence			
M_{c0}	p_{cLN}	$K\alpha c$	τ	p_{cLN}	αc	$2K$
0.5	1.848	684	0.687	1.848	7.83	175
0.55	1.385	293	0.544	1.385	5.19	113
0.6	1.036	138	0.427	1.036	3.47	79.3
0.65	0.766	67.1	0.329	0.766	2.33	57.7
0.7	0.555	33.8	0.247	0.555	1.54	44.0
0.75	0.390	18.9	0.179	0.390	0.996	37.9
0.8	0.261	10.6	0.123	0.261	0.620	34.1
0.9	0.082	3.35	0.040	0.082	0.174	38.5

PART II

Summary.—The method given in Part I of calculating a first approximation to the ideal theoretical drag rise due to a shock wave on an aerofoil is extended to cover the use of the Kármán-Tsien solution in place of the Glauert relation. It is shown how the drag rise can be calculated from the theoretical critical Mach number and the geometrical curvature of the surface at the point of maximum suction. In particular for two aerofoils having the same critical Mach number the drag rise is proportional to the radius of curvature; thus the drag rise on a 17.3% ellipse at zero incidence will be three times that for an NACA 0012 section having the same critical Mach number.

Comparison with experiment in the N.P.L. 20 in × 8 in High-Speed Tunnel shows that for a number of aerofoil shapes the theoretical rise occurs consistently from $M = 0.1$ to 0.13 later than the observed rise.

The present method is simple and should give at least a better indication of the relative merits of different aerofoil shapes than a knowledge of the theoretical critical speed alone.

In A.R.C. 5958¹, and Part I of this paper, a method was advanced of calculating the drag of an aerofoil arising from the increase of entropy through a limited shock wave, on the basis of some rather crude assumptions. In outline these assumptions were as follows.

1. The shock wave starts from the point of maximum velocity on the upper surface as calculated for incompressible flow and follows the course of the low-speed equipotential through this point.
2. The velocity just upstream of the shock wave is deduced from the low Mach number potential field by means of one of the standard assumptions (in the previous reports¹ and Part I of this paper, by the Glauert relation as applied by Jacobs and alternatively in the present report by the Kármán-Tsien relation).
3. The shock wave occurs whenever the maximum velocity exceeds the local velocity of sound and ends at the point at which $M = 1$, as deduced from assumption 2.

Calculations were made in A.R.C. 5958¹ on the basis of the above assumptions for two elliptic cylinders at zero incidence and for an aerofoil shape at two values of incidence. These calculations involve no further simplifying assumptions.

In Part I the increase of C_D due to the shock wave was treated as an expansion in positive powers of $(M_0 - M_{c0})$, where M_0 is the actual free-stream Mach number and M_{c0} is the free-stream Mach number at which the velocity of sound is first attained on the surface. It was shown that the first term of the expansion involves the fourth power of $(M_0 - M_{c0})$. The value of the coefficient K in the relation

$$C_D = K(M_0 - M_{c0})^4 + 0(M_0 - M_{c0})^5 \quad \dots \quad (1)$$

was evaluated in a general manner as a function of M_{c0} and α , where α is the coefficient of s in the expansion

$$p_{cL} = p_{cLN} - \alpha s + 0(s^2) \quad \dots \quad (2)$$

p_{cL} ($= -p/\frac{1}{2}\rho V^2$) is the suction coefficient in potential flow at low Mach number at a point at distance s from the surface of the body along the equipotential line through the point N of maximum velocity, p_{cLN} being the value of p_{cL} at this point. Thus a knowledge of the values of M_{c0} and K gives a first approximation to the entropy drag.

The numerical value of K was calculated for the general case of the elliptic cylinder at zero incidence.

It has since been noticed that the value of α can be expressed as a function of M_{c0} (or p_{cLN}) and of the geometrical curvature of the surface at the point N, by the formula

$$\alpha c = (2c/R) (1 + p_{cLN}) \quad \dots \quad (3)$$

This is demonstrated in Appendix A, or it could be deduced from the relation between centrifugal force and curvature in a curved stream. It would therefore be a simple matter to determine K for any shape or incidence for which the theoretical value of M_{c0} (or p_{cLN}) is known, provided that the shape can be expressed as a reasonably simple algebraical formula (or a rough value can be obtained from the plotted shape). The method of Ref. 1 on the other hand is too laborious for extensive use.

The opportunity has also been taken of generalising the formulae slightly, so as to cover the type of relation between compressible and incompressible suction coefficient given by Kármán and Tsien. This generalisation is made in Appendix B, which also contains the explicit results arising both from the Glauert-Jacobs relation, as in Part I and from the Kármán-Tsien relation.

In Part I the relation between compressible suction coefficient p_c and incompressible coefficient p_{cL} was assumed to be of the form

$$p_c = p_{cL} \phi(M_0),$$

where M_0 is the Mach number of the free stream. This has been generalised into the form

$$p_c = \Phi(p_{cL}, M_0),$$

which covers the Kármán-Tsien relation.

It is shown in Part I that the formula for the coefficient K in terms of α and M_{c0} (for a given form of relation between p_{cLN} and M_{c0}) is of the form $\alpha cK = \text{Function of } M_{c0} \text{ only}$. Values of αcK have been tabulated in Table 2b both for the Glauert and for the Kármán relation; the former supersedes Table 1 of Part I which is not very accurate; the corresponding relations between p_{cLN} and M_{c0} are given in Table 2a. From Table 2b, values of K can be deduced when p_{cLN} and α are known, the latter being deduced from the geometrical curvature by use of equation (A8) of Appendix A.

Additional arguments in favour of the use of (1) are:—

1. The basic assumptions become less and less justifiable as $M_0 - M_{c0}$ increases from zero, so that it is doubtful whether it is worth while to go beyond a first order theory.

2. Fig. 3 (reproduced from Fig. 2 of Ref. 1) shows that for two elliptic cylinders at zero incidence, the first approximation of Part I agrees reasonably well with the calculations of Ref. 1*.

In Table 3 are given values of M_{c0} and K calculated by the formulae of the Appendices using the Kármán relation for a number of typical aerofoils; values of M_{c0} range from 0.65 to 0.8. Curves of ΔC_D , calculated for a selection of these aerofoils by Formula 1, are given in Fig. 4a. The value of ΔC_D is taken as the sum of the values for the upper and lower surfaces calculated separately.

An interesting comparison is that between NACA 0020 and the 20 per cent ellipse, both at zero incidence. The value of M_{c0} for the latter, exceeds that for the former by 0.058, but the difference of the values of M_{c0} for a ΔC_D of 0.02 is only 0.023; thus the advantage of the ellipse gets smaller as the drag rises. Although this comparison does not include the effect of breakaway, it may help to explain the rather disappointing results of attempts to reduce shock stalling effects by improving the shape of a section leaving the thickness unaltered.

Table 3 also illustrates the fact that for two aerofoils (symmetrical and at zero incidence) of different shape and thickness having the same critical speed, the ratio of the drag rises is equal to the ratio of the radii of curvature. Thus the drag rise for a 17.3 per cent. ellipse is three times that for the 0012 section which has the same critical Mach number.

* The Glauert relation is used in both cases.

In Fig. 4b some of the calculated values of ΔC_D are compared with values of profile drag measured in the N.P.L. Rectangular High Speed Tunnel (details are given in Appendix C). In all cases the theoretical value of ΔC_D has been increased by the approximate amount of the observed value below the shock stall.

It is remarkable that the difference between the calculated ideal drag rise and the rise observed in the tunnel can be represented by a change of Mach number which lies between 0.10 and 0.13 for four very diverse cases. Apart from errors in the theoretical curves due to the approximations employed, this difference has been commonly attributed to a breakaway of the boundary layer caused by the shock wave. Of other possible causes of discrepancy, tunnel interference should be small, since the flexible walls of the rectangular tunnel were shaped to agree with free streamlines by the method of A.R.C. 8073².

The curve of the flight results on NACA 2218 ('Tornado'), derived from A.R.C. 5990⁷, though of very limited extent, might suggest that the breakaway in flight is about one half of that occurring on the model; similar results of diving tests on the 'Mustang' and 'Spitfire' will be of the greatest interest.

Humidity is another possible factor tending to give a spuriously high drag coefficient in the N.P.L. tunnels which might account for a part of the discrepancy.

In a recent report, A.R.C. 8286, Monaghan and Fowler have calculated the drag corresponding to the irreversible loss through a shock wave on the basis of measured static pressures near the shock wave on an aerofoil in the N.P.L. rectangular high-speed tunnel. In the case considered the corresponding drag values based on the assumptions of the present paper were seriously in error, so that at a Mach number slightly more than 0.1 above the critical the rise of drag coefficient as calculated by the formulae of the present paper occurs at a Mach number about 0.05 higher than the same value as based on observed static pressures, and the latter again at about 0.05 higher than the same value as measured in the tunnel by pitot traverse. The extreme difference of 0.1 agrees with the other cases illustrated in Fig. 2.

If it were legitimate to argue from a cross comparison of two different aerofoils (a modern shape 14.5 per cent. thick of A.R.C. 8286⁴ and NACA 2218 of Fig. 3) it might be suggested that there is no appreciable breakaway in flight, the drag agreeing with that calculated from the pressures near the shock wave on the model.

In general the results suggest that the present method may give a better indication of the relative merits of different aerofoil sections than is given by the theoretical critical speed above and that it would be worth while to undertake the small extra labour of calculating the factor K whenever the theoretical critical speed is calculated.

APPENDIX A

Determination of the Coefficient α of Equation (2) in Terms of the Geometrical Curvature

Take as origin 0 the point of maximum suction on the surface of a body in two dimensions (incompressible fluid); take axes $0x$ tangential to the surface downstream and $0y$ normal into the fluid. Then since the total velocity q is stationary at the origin and parallel to the axis of x , we can write,

$$u - iv = q_0 + ib_1z + 0(r^2), \quad \dots \quad (A1)$$

and so
$$\psi = q_0y + \frac{1}{2}b_1(x^2 - y^2) + 0(r^3), \quad \dots \quad (A2)$$

$$u = q_0 - b_1y + 0(r^2), \quad \dots \quad (A3)$$

where
$$r^2 = x^2 + y^2.$$

If p_1 is the pressure just in front of a shock wave (assumed normal to the local streamlines) and M_1 the Mach number at the same point, it follows from the ordinary adiabatic relation that

$$1 + \frac{1}{2} (\gamma - 1) M_1^2 = \{1 + \frac{1}{2} (\gamma - 1) M_0^2\} (p_1/p_0)^{-\frac{\gamma-1}{\gamma}}, \dots \dots \dots (13, \text{Part I})$$

while it follows from (B1) on putting $\frac{1}{2} p_0 V^2 = \frac{1}{2} \gamma p_0 M_0^2$

that
$$p_1/p_0 = 1 - \frac{1}{2} \gamma M_0^2 \Phi (p_{cL}, M_0), \dots \dots \dots (B3)$$

which takes the place of (12, Part I). At the point of maximum suction N (at which $p_{cL} = p_{cLN}$) and at the free-stream Mach number (M_{c0}) at which the velocity of sound is first attained, a relation between M_{c0} and p_{cLN} can be deduced by putting $M_1 = 1$ in (13, Part I) and eliminating p_1/p_0 between (3, Part I) and (B3).

The formulae of (Part I) Appendix 1 are then modified as follows. Writing as before μ_{1M} and μ_{1p} for the result of differentiating the value of M_1 deducible from (13, Part I) and (B3) with respect to M_0 and p_{cL} respectively and then putting $M_1 = 1$, $M_0 = M_{c0}$, $p_{cL} = p_{cLN}$, after differentiation, we find

$$\mu_{1M} = \frac{1}{2} (\gamma + 1) M_{c0} \left\{ \frac{1}{1 + \frac{1}{2} (\gamma - 1) M_{c0}^2} + \left(\frac{p_0}{p_1} \right)_N \Phi_A \right\}, \dots \dots (B4)$$

where
$$\Phi_A = \Phi + \frac{1}{2} M_{c0} \Phi_M, \dots \dots \dots (B5)$$

and
$$\mu_{1p} = \frac{1}{4} (\gamma + 1) \left(\frac{p_0}{p_1} \right)_N M_{c0}^2 \Phi_p, \dots \dots \dots (B6)$$

where Φ_M and Φ_p stand for the result of putting $M_0 = M_c$ and $p_{cL} = p_{cLN}$ in $\partial\Phi/\partial M_0$ and $\partial\Phi/\partial p_{cL}$ after differentiation. The formula for K then becomes

$$\alpha cK = \frac{2 (\gamma + 1) (p_1/p_0)^{(3\gamma+1)/2\gamma}}{3 M_{c0} \Phi_p} \left\{ \frac{1}{1 + \frac{1}{2} (\gamma - 1) M_{c0}^2} + \frac{p_0}{p_1} \cdot \Phi_A \right\}^4 \dots \dots (B7)$$

On substituting the Kármán-Tsien relation (B3) for (B1) we have

$$\begin{aligned} \Phi_M &= \beta^{-2} \{1 + \frac{1}{2} \Phi\} \Phi M_{c0}, \\ \Phi_A &= \beta^{-2} \Phi \{1 - \frac{1}{2} M_{c0}^2 (1 - \frac{1}{2} \Phi)\}, \\ \Phi_p &= \beta (\Phi/p_{cLN})^2. \end{aligned}$$

For the Glauert-Jacobs relation,

$$\begin{aligned} \Phi_M &= \beta^{-2} M_c \Phi, \\ \Phi_A &= (1 - \frac{1}{2} M_{c0}^2) \beta^{-2} \Phi, \\ \Phi_p &= \beta^{-1}. \end{aligned}$$

APPENDIX C

Notes on Fig. 2b, Experimental Curves, Drag Coefficient by Pitot Traverse Method

- Mustang Section : 5-in chord model in 20-in \times 8-in High Speed Tunnel at N.P.L. A.R.C. 8135⁵.
 NACA 2218 ('Tornado') : 5-in chord model in 20-in \times 8-in tunnel. A.R.C. 6661⁶.
 NACA 2218 ('Tornado') : Flight experiment. A.R.C. 5990⁷.
 EC 1250 : 5-in chord model in 20-in \times 8-in tunnel. Not yet issued⁸. (Compared with theoretical curve for 12 per cent. ellipse).
 NACA 0020 : 2-in chord in 20-in \times 8-in tunnel. Not yet issued⁸.
 Circular High Speed Tunnel. 4709⁹.
 5-in \times 2-in tunnel. 7153¹⁰.

All experimental curves are subject to an unknown correction (in the direction of increased Mach number for given C_D), for the effect of condensation of moisture. This will be less for the 5-in \times 2-in tunnel and may in part account for the discrepancy between this tunnel and the other two for the NACA 0020 section.

Critical Mach numbers are indicated by arrows ; values for 'Mustang' are derived from pressure observation ; the remainder are calculated.

REFERENCES

<i>No.</i>	<i>Author</i>	<i>Title, etc.</i>
1	P. R. Owen and A. D. Young	Note on the Drag Effect of Shock Waves. A.R.C. 5958.
2	Th. von. Kármán	Compressibility Effects in Aerodynamics. From "Journal of the Aeronautical Sciences". July, 1941. A.R.C. 5314.
3	C. N. H. Lock and J. A. Beavan	Tunnel Interference at Compressibility Speeds using the Flexible Walls of the Rectangular High Speed Tunnel. R. & M. 2005. 1944.
4	R. J. Monaghan and R. G. Fowler	An Estimate, Based on Experimental Data, of the Ideal Drag of a Shock Wave. A.R.C. 8286. (To be published.)
5	J. S. Thompson, M. Markowicz, J. A. Beavan and R. G. Fowler.	Pressure Distribution and Wake Traverses on Models of 'Mustang' Wing Section in the R.A.E. and N.P.L. High Speed Tunnels. R. & M. 2251. August, 1944.
6	H. H. Pearcey	Drag Measurements on N.A.C.A. 2218 Section at Compressibility Speeds for Comparison with Flight Tests and Theory. R. & M. 2093. April, 1943.
7	W. A. Mair	Flight Measurements of Profile Drag at High Speeds. A.R.C. 5990. (To be published.)
8	J. A. Beavan	Note on Rise of Drag above the Critical Mach Number. (Unpublished.)
9	C. N. H. Lock, W. F. Hilton and S. Goldstein.	Determination of Profile Drag at High Speeds by a Pitot Traverse Method. R. & M. 1971. September, 1940.
10	A. Fage and R. F. Sargent	Effect on Aerofoil Drag of Boundary Layer Suction behind a Shock Wave. R. & M. 1913. October, 1943.

TABLE 2a
Values of M_{c0} and p_{cLN}

	Kármán	Glauert
M_{c0}	P_{cLN}	P_{cLN}
0.50	1.6170	1.8476
0.55	1.2184	1.3849
0.60	0.91680	1.03546
0.625	0.79300	0.89244
0.65	0.68365	0.76641
0.675	0.58675	0.65504
0.70	0.50062	0.55636
0.725	0.42391	0.46881
0.75	0.35546	0.39103
0.775	0.29440	0.32200
0.80	0.23993	0.26078
0.85	0.14487	0.15908

TABLE 2b
Values αcK for given M

<i>Kármán</i>				<i>Kármán</i>			
M	log αcK	αcK	Diff.	M	log αcK	αcK	Diff.
0.50	2.92066	833.03		0.675	1.73021	53.729	
	2.88125	760.76	72.276		1.70082	50.214	3.515
	2.84222	695.38	65.38		1.67162	46.948	3.266
	2.80355	636.14	59.24		1.64262	43.916	3.032
0.525	2.76525	582.44	53.70	0.700	1.61382	41.098	2.818
	2.72731	533.72	48.72		1.58520	38.477	2.621
	2.68975	489.50	44.22		1.55677	36.039	2.438
	2.65254	449.30	40.19		1.52851	33.768	2.271
0.55	2.61568	412.74	36.56	0.725	1.50043	31.654	2.114
	2.57916	379.45	33.29		1.47251	29.683	2.071
	2.54296	349.11	30.34		1.44476	27.846	1.837
	2.50708	321.42	27.68		1.41717	26.132	1.714
0.575	2.47154	296.17	25.26	0.75	1.38973	24.532	1.600
	2.43632	273.10	23.07		1.36246	23.039	1.493
	2.40140	252.00	21.10		1.33533	21.644	1.395
	2.36678	232.69	19.31		1.30834	20.339	1.305
0.600	2.33248	215.02	17.67	0.775	1.28149	19.120	1.219
	2.29846	198.82	16.20		1.25477	17.979	1.141
	2.26472	183.96	14.86		1.22817	16.911	1.068
	2.23125	170.31	13.64		1.20171	15.911	1.000
0.625	2.19806	157.78	12.53	0.8	1.17537	14.975	0.936
	2.16515	146.26	11.52		1.14914	14.097	0.878
	2.13250	135.67	10.59		1.12299	13.274	0.823
	2.10011	125.92	9.75		1.09694	12.501	0.773
0.650	2.06798	116.94	8.98	0.825	1.07098	11.776	0.725
	2.03611	108.67	8.27		1.04509	11.094	0.682
	2.00448	101.04	7.63		1.01928	10.454	0.640
	1.97309	93.992	7.045		0.99354	9.8524	0.602
0.675	1.94194	87.486	6.505	0.85	0.96785	9.2865	0.566
	1.91102	81.474	6.012		0.94221	8.7541	0.532
	1.88034	75.917	5.557		0.91661	8.2530	0.501
	1.84988	70.775	5.142		0.89103	7.7810	0.472
0.675	1.81964	66.015	4.760	0.85	0.86548	7.3364	0.445
	1.78962	61.606	4.409		0.83995	6.9176	0.419
	1.75981	57.519	4.087		0.81444	6.5229	0.395
	1.73021	53.729	3.790		0.78894	6.1509	0.372

TABLE 2b (contd.)

<i>Glauert</i>				<i>Glauert</i>			
<i>M</i>	<i>log acK</i>	<i>acK</i>	<i>Diff.</i>	<i>M</i>	<i>log acK</i>	<i>acK</i>	<i>Diff.</i>
0.50	2.83507	684.02	57.88	0.675	1.68243	48.132	3.032
	2.79667	626.14	52.49		1.65417	45.100	2.821
	2.75865	573.65	47.62		1.62612	42.279	2.627
	2.72101	526.03	43.26		1.59826	39.652	2.448
0.525	2.68374	482.77	39.72	0.700	1.57059	37.204	2.283
	2.64684	443.45	35.79		1.54309	34.921	2.128
	2.61030	407.66	32.57		1.51578	32.793	1.986
	2.57413	375.09	29.71		1.48865	30.807	1.854
0.550	2.53830	345.38	27.09	0.725	1.46170	28.953	1.731
	2.50282	318.39	24.75		1.43492	27.222	1.618
	2.46767	293.54	22.61		1.40830	25.604	1.514
	2.43285	270.93	20.69		1.38184	24.090	1.416
0.575	2.39836	250.24	18.94	0.750	1.35553	22.674	1.325
	2.36418	231.30	17.34		1.32938	21.349	1.241
	2.33033	213.96	15.91		1.30337	20.108	1.163
	2.29677	198.05	14.60		1.27749	18.945	1.090
0.600	2.26352	183.45	13.41	0.775	1.25176	17.855	1.022
	2.23056	170.04	12.31		1.22615	16.833	0.960
	2.19790	157.73	11.33		1.20066	15.873	0.901
	2.16554	146.40	10.43		1.17528	14.972	0.846
0.625	2.13345	135.97	9.60	0.800	1.15001	14.126	0.795
	2.10166	126.37	8.85		1.12485	13.331	0.748
	2.07011	117.52	8.18		1.09977	12.583	0.704
	2.03879	109.34	7.53		1.07478	11.879	0.662
0.650	2.00777	101.81	6.963	0.825	1.04987	11.217	0.624
	1.97702	94.847	6.435		1.02503	10.593	0.587
	1.94651	88.412	5.952		1.00025	10.006	0.5537
	1.91624	82.460	5.509		0.97553	9.4523	0.5223
0.675	1.88621	76.951	5.102	0.850	0.95085	8.9300	0.4927
	1.85642	71.849	4.724		0.92620	8.4373	0.4653
	1.82688	67.125	4.384		0.90156	7.9720	0.4396
	1.79755	62.741	4.065		0.87693	7.5324	0.4151
0.675	1.76846	58.676	3.776	0.850	0.85231	7.1173	0.3921
	1.73957	54.900	3.507		0.82770	6.7252	0.3705
	1.71090	51.393	3.261		0.80309	6.3547	0.3500
	1.68243	48.132			0.77849	6.0047	

TABLE 3
Ideal Drag Rise Summary

Wing	Incidence or C_L	$\frac{p_{eLN}}{-C_{p0}}$	at $\frac{x}{c} =$	$\frac{c}{R}$	M_{e0}	αc	K
'Mustang' U.S. } L.S. }	0°	{ 0.512 0.256	0.4	1.0*	0.697 ⁽¹⁾	3.024	13.22
12% Ellipse	0°	0.2544	0.161	2.34	0.632 ⁽²⁾	8.25	11.88
NACA 0020	0°	0.663	0.5	0.24	0.793 ⁽²⁾	0.602	20.18
NACA 0012	0°	0.663	0.151	1.67	0.655 ⁽²⁾	5.56	12.65
NACA 0012	0°	0.375	0.151	1.030	0.742 ⁽²⁾	2.83	7.95

* Approximate values by interpolation.

⁽¹⁾ From observed pressures.

⁽²⁾ By calculation.

U.S. Upper surface.

L.S. Lower surface.

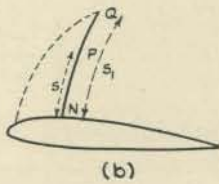
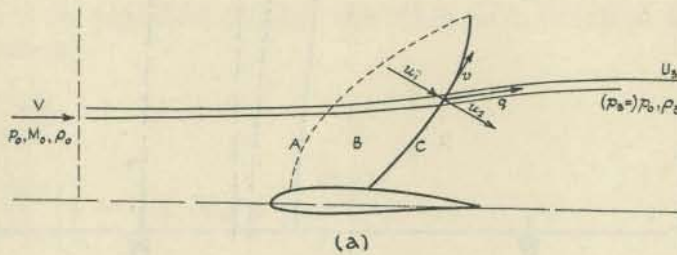


FIG. 1.

— Theoretical.

--- Experimental

Form drag from pressure plotting in N.A.C.A. high speed tunnel.
 Total drag deduced from wake exploration at N.P.L.

Vertical arrows denote critical Mach numbers.

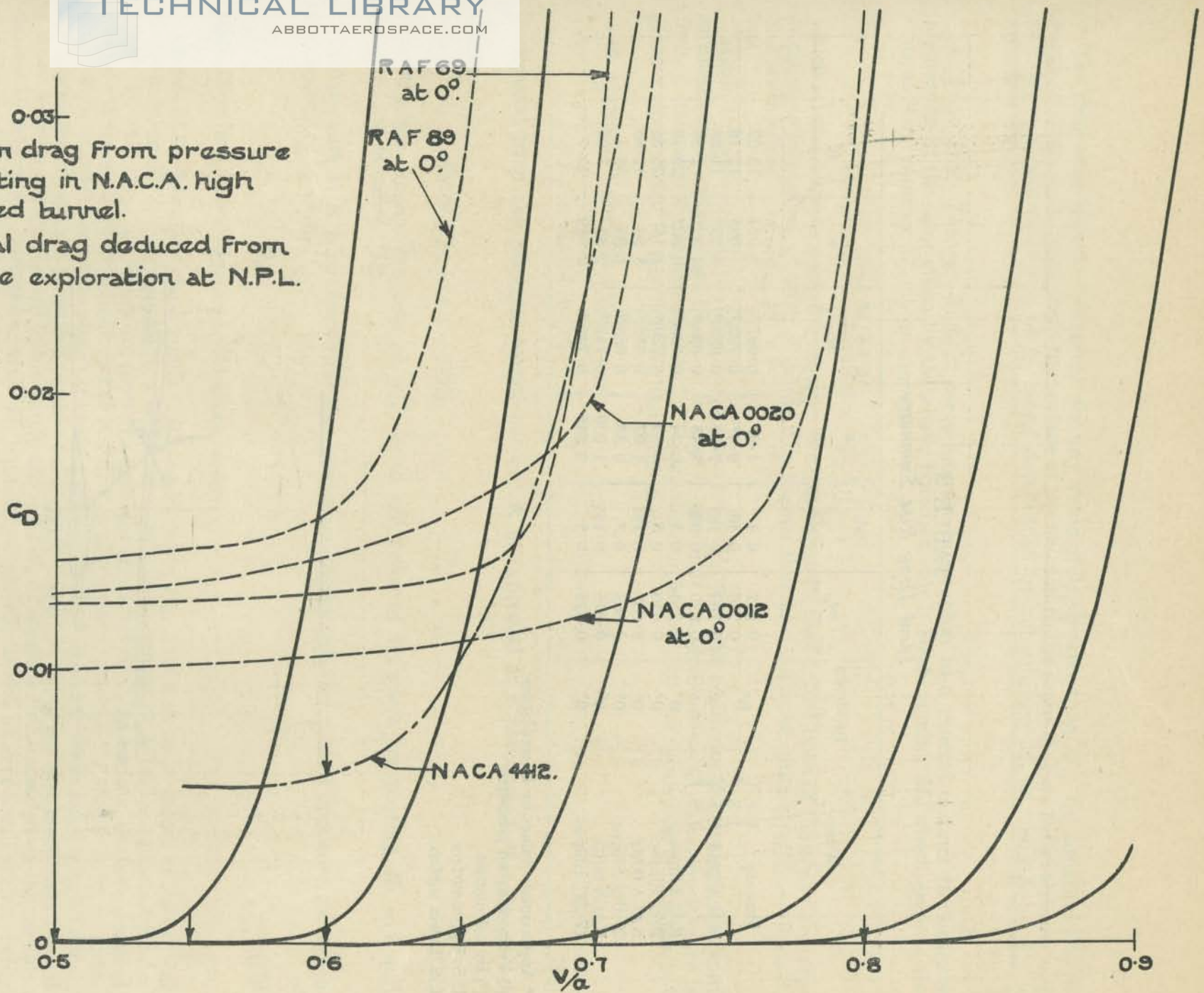


FIG. 2. Theoretical Increase of Drag Produced by Local Shock Waves.

16

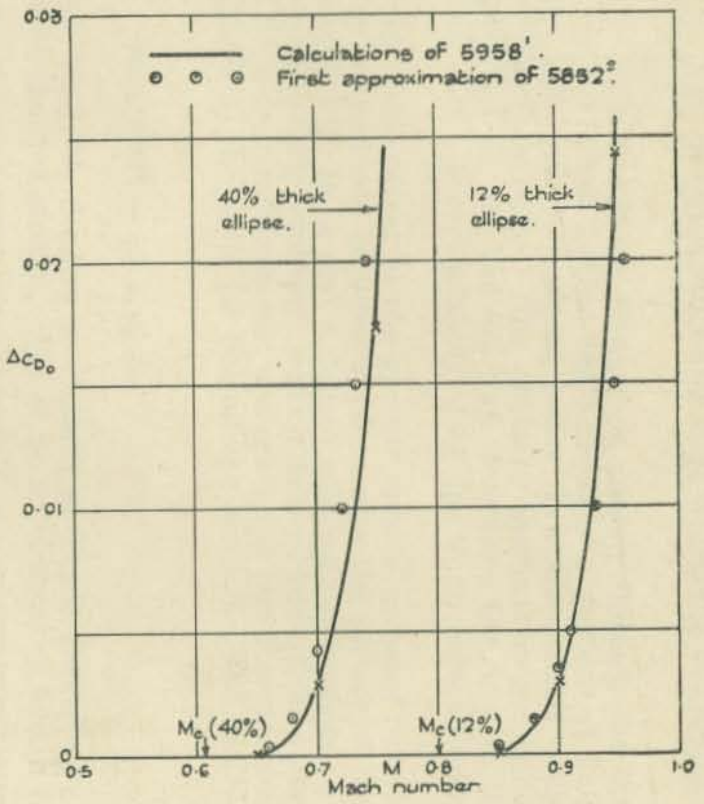


FIG. 3. Theoretical Variation of Drag Increment Due to Shock Waves with Mach Number for 12 per cent. Thick and 40 per cent. Thick Ellipses.

— Calculations of 5958¹
 ○ ○ ○ First approximation of Part I.

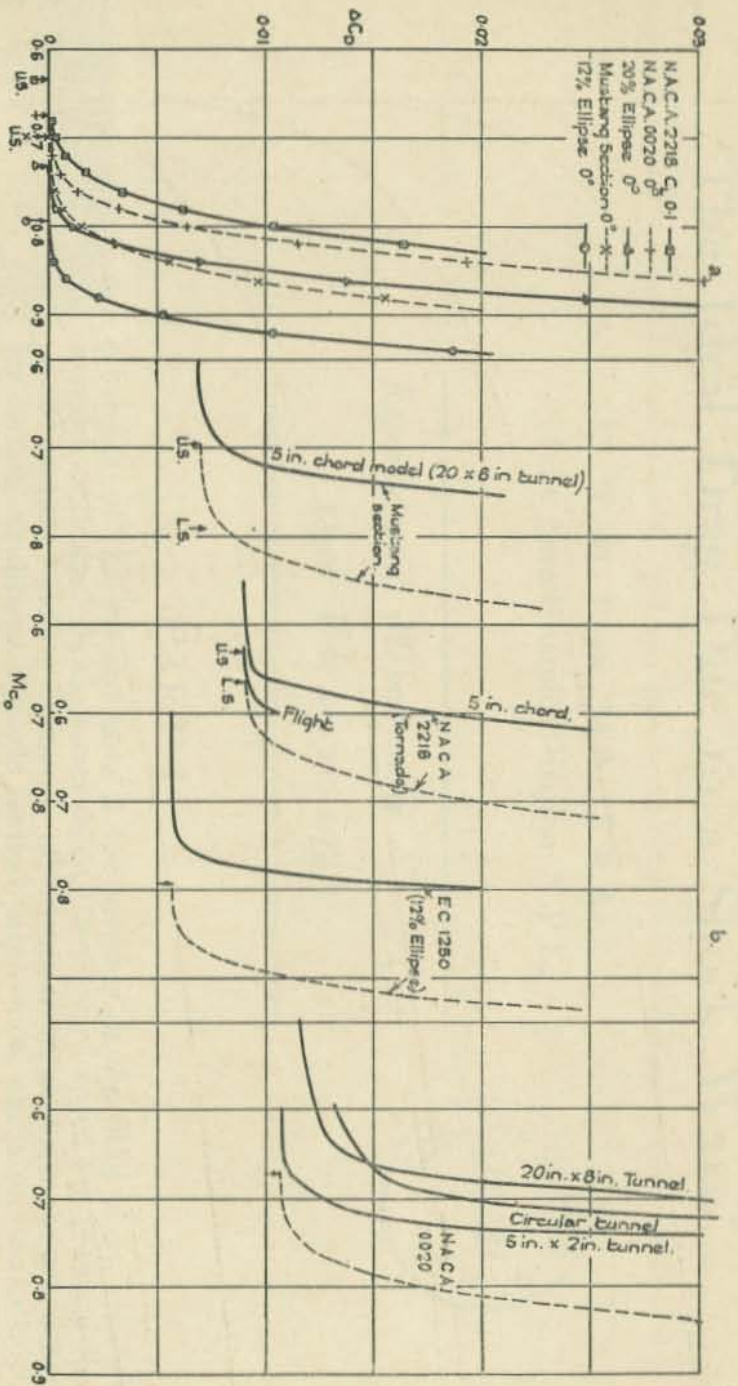


FIG. 4. Ideal drag rise (first approximation) Experimental (pilot traverse)